# 5. PROPELLER THEORIES

a) Momentum Theory

It was originally intended to provide an analytical means for evaluating ship propellers (Rankine 1865 & Froude 1885). Momentum Theory is also well known as Disk Actuator Theory. Momentum Theory assumes that

- the flow is inviscid and steady (ideal flow), therefore the propeller does not experience energy losses due to frictional drag
- also the rotor is thought of as an actuator disk with an infinite number of blades, each with an infinite aspect ratio
- the propeller can produce thrust without causing rotation in the slipstream.
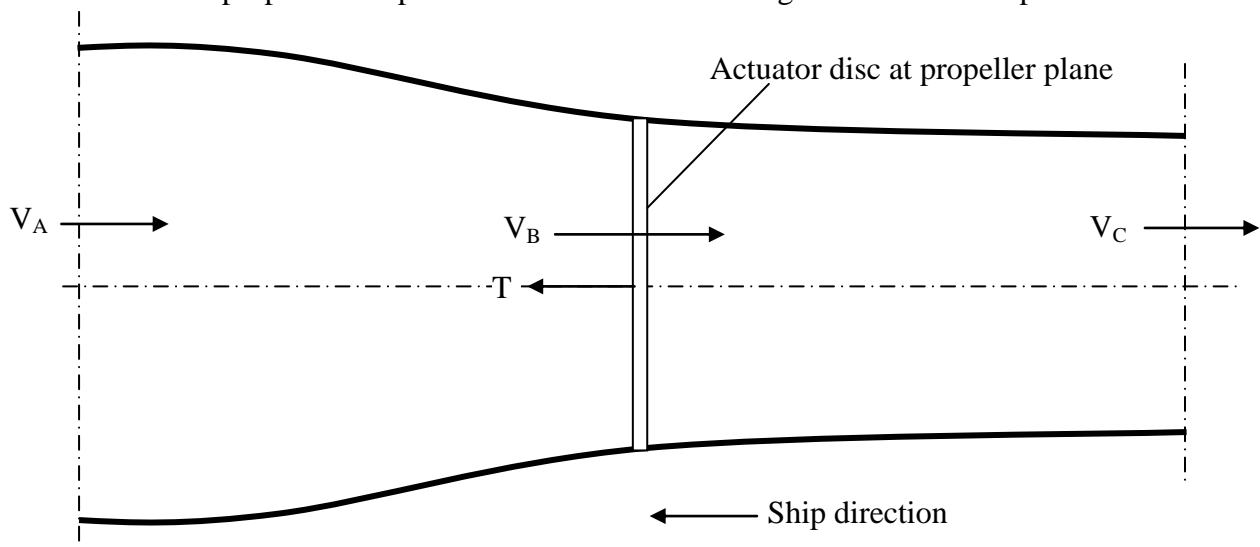
From the basic thrust equation, we know that the amount of thrust depends on the mass flow rate through the propeller and the velocity change through the propulsion system. In the above figure the flow is proceeding from left to right. Let us denote the subscripts "A and C" for the stations assumed to be far upstream and downstream of the propeller respectively and the location of the actuator disc by the subscript "B".

The thrust (T) is equal to the mass flow rate ($\dot{m}$) times the difference in velocity (V).

$$T = \dot{m}(V_C - V_A) \tag{1}$$

There is no pressure-area term because the pressure at the C is equal to the pressure at A.

The power P_D absorbed by the propeller is given by:

$$P_D = \frac{1}{2}\dot{m}(V_C^2 - V_A^2) \tag{2}$$

$$\dot{m} = \rho A V \,(kg/s)$$

However delivered power P_D is also equal to the work done by thrust force:

$$P_D = TV_B \tag{3}$$

By equating Eqs. (2) and (3), the velocity at the propeller position becomes:

$$V_B = \frac{1}{2}(V_C + V_A) \tag{4}$$

If V_B and V_C are expressed in terms of the velocity V_A, then:

$$\begin{aligned} V_B &= V_A + u_a \\ V_C &= V_A + u_{a1} \end{aligned} \tag{5}$$

where u_a and u_{a1} are known as the increases in the velocities at the propeller disc position B and C.

As a consequence the slipstream must contract between the conditions existing far upstream and those existing downstream in order to satisfy the continuity equation:

$$\begin{aligned} &Q_A = Q_B = Q_C \text{ volume flow rate} (m^3/s) \\ &V_A A_A = V_B A_B = V_C A_C \\ &V_A A_A = (V_A + u_a)A_B = (V_A + u_{a1})A_C \end{aligned} \tag{6}$$

where

$$A_A = \frac{\pi D_A^2}{4}, A_B = \frac{\pi D^2}{4} \text{ and } A_C = \frac{\pi D_C^2}{4}$$

We can obtain that:

$$\begin{aligned} D_A^2 &= \frac{V_A + u_a}{V_A}D^2 \\ D_C^2 &= \frac{V_A + u_a}{V_A + u_{a1}}D^2 \end{aligned} \tag{7}$$

The law of conservation of momentum equates the force exerted on the fluid with the net outflow of momentum. The control volume is the stream tube from A_A to A_C. The mass per unit time through A_A is $\rho V_A A_A$ and the momentum inflow is $\rho V_A^2 A_A$. Similarly the momentum outflow through A_C can be written and the conservation of momentum requires that:

$$\rho V_A^2 A_A - \rho(V_A + u_{a1})^2 A_C + T = 0 \tag{8}$$

Using Eq. (7) this can be written as:

$$T = \frac{\pi}{4} D^2 \rho (V_A + u_a) u_{a1} \tag{9}$$

The thrust can also be written as T=ΔpA

We can use Bernoulli's equation to relate the pressure and velocity upstream and downstream of the propeller disk, but not through the disk. For the upstream and downstream of the disk, respectively:

$$\frac{1}{2} \rho V_A^2 + p_A = \frac{1}{2} \rho (V_A + u_a)^2 + p_B$$
$$\frac{1}{2} \rho (V_A + u_{a1})^2 + p_C = \frac{1}{2} \rho (V_A + u_a)^2 + p_B + \Delta p \tag{10}$$

p$_A$=p$_C$

Subtracting the above equations gives:

$$\Delta p = \frac{1}{2} \rho (2 V_A u_{a1} + u_{a1}^2) \tag{11}$$

A second formulation for the propeller thrust is:

$$T = \frac{\pi}{4} D^2 \rho (V_A + \frac{u_{a1}}{2}) u_{a1} \tag{12}$$

Then combining Eqs. (9) and (12) it is derived that:

$$u_{a1} = 2 u_a \tag{13}$$

This shows that half of the acceleration takes place before the propeller disc and the remaining half after the propeller disc. In other words the axial induced velocity at the propeller (u_a) is the half the axial induced velocity at the C.

The relation between the propeller thrust and the axial induced velocity is:

$$T = \frac{\pi}{4} D^2 \rho (V_A + u_a) 2 u_a \tag{14}$$

The propeller thrust is made non-dimensional with the propeller area and the inflow velocity V$_A$:

$$C_T = \frac{T}{\frac{\pi}{4} D^2 \frac{1}{2} \rho V_A^2} \tag{15}$$

where C_T is a thrust coefficient indicating the propeller loading. Eq. (15) becomes

$$C_T = 4\frac{u_a}{V_A}(1+\frac{u_a}{V_A})$$

or   (16)

$$\frac{u_a}{V_A} = -\frac{1}{2} + \frac{1}{2}\sqrt{1+C_T}$$

The induced velocity in the slipstream represents energy supplied to the flow behind the propeller. This is due to the fact that the fluid gives way when a thrust is exerted to it. The loss of the energy is reflected in an efficiency which is lower than 1. To formulate the efficiency the propeller disk moves with a velocity V_A and exerts a force T. The power is TV_A. In the slipstream a velocity $2u_a$ is present. With the mass flow expressed as the mass flowing through the propeller disk, which is equal to that flowing through the slipstream, this represents an energy of:

$$E_{lost} = \rho(V_A + u_a)(\frac{\pi}{4}D^2)(2u_a)^2$$ (17)

The efficiency of the propeller can be written as:

$$\eta_0 = \frac{TV_A}{TV_A + E_{lost}}$$ (18)

By inserting Eq. (17) into (18) gives:

$$\eta_0 = \frac{1}{1+\dfrac{u_a}{V_A}}$$

*or*   (19)

$$\eta_0 = \eta_i = \frac{2}{1+\sqrt{1+C_T}}$$

This represents the maximum efficiency which is theoretically possible in an inviscid flow with a propeller not introducing any rotation in the slipstream. It is therefore called the ideal efficiency.


b) Blade Element Theory

The primary limitation of the *momentum theory* is that it provides no information as to how the rotor blades should be *designed* so as to produce a given thrust. Also, profile *drag losses are ignored*. The blade-element theory is based on the assumption that each element of a propeller or rotor can be considered as an *airfoil segment. Lift and drag* are then calculated from the *resultant velocity acting on the airfoil*, each element considered independent of the adjoining elements. The *thrust and torque* of the rotor

are obtained by *integrating* the individual contribution of each element along the radius.
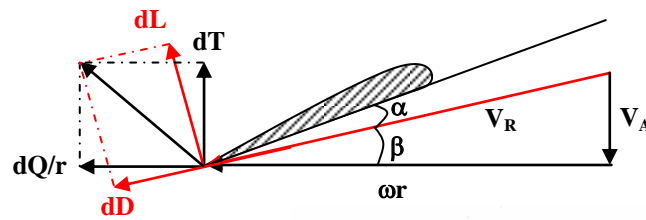
where

dT: Trust
dQ: Torque
dL: Lift
dD: Drag
V_A: Advanced velocity
ωr: Rotational speed
V_R: Resultant velocity
α: Angle of attack
β: Hydrodynamic pitch angle
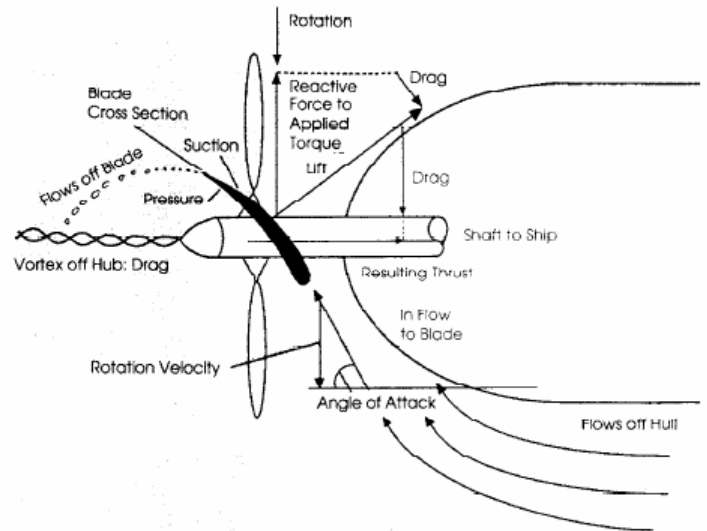
V_R is defined as:

$$V_R = \sqrt{V_A^2 + (\omega r)^2}$$

The thrust force of a blade can be obtained by integrating the dT over the radius R and the total thrust force is found by the multiplication of number of blades by the blade thrust force.

$$T = Z\int_{r_h}^{R} dTdr = Z\int_{r_h}^{R}(dL\cos\beta - dD\sin\beta)dr \tag{20}$$

Similarly total torque can be obtained as:

$$Q = Z\int_{r_h}^{R} dQdr = Z\int_{r_h}^{R} dFrdr = Z\int_{r_h}^{R}(dL\sin\beta + dD\cos\beta)rdr \tag{21}$$

The propeller efficiency:

$$\eta = \frac{TV_A}{Q\omega} \tag{22}$$

c) Profile Characteristics

A characteristic feature of a profile is to generate lift (L). This profile (lifting surface) in a flow also generates drag (D) and pitching moment (M). The lift is caused by the fact that the flow is forced to leave the profile smoothly at the tail. This is in turn an effect of viscosity which prevents the velocities from becoming extremely large at the tail. This condition is called Kutta condition. Basically it is a tangential flow at the tail, or equal pressure at both sides of the tail.

Consider a profile moving at a certain angle of attack through the fluid as in the figure below.
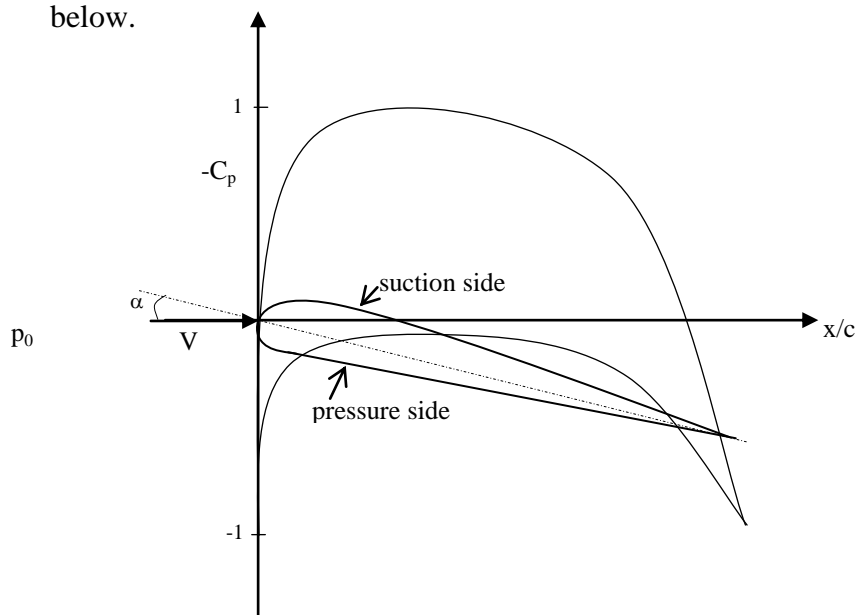
There is an inflow velocity at the angle of attack α. As a result of the inflow there is a certain pressure distribution over the surface of the profile. When the pressure p_0 in the undistributed flow is changed, the pressure over the surface of the profile will also change with the same amount. The pressure is made non-dimensional as:

$$C_p = \frac{p - p_0}{\frac{1}{2}\rho V^2} \tag{23}$$

In the flow the Bernoulli Law is valid so the pressure distribution at the surface of the profile can be related to the local velocity v by:

$$p + \frac{1}{2}\rho v^2 = p_0 + \frac{1}{2}\rho V^2 \tag{24}$$

The effect of the immersion h is neglected, because the profile is assumed to be nearly horizontal and a small angle of attack. The above equation can be written as:

$$C_p = 1 - (\frac{v}{V})^2 \tag{25}$$

The above equation shows that two stagnation points exist where the local velocity is zero. These stagnation points are called forward and rear stagnation points. Typical pressure distribution on a profile is shown in the above figure.

The pressure difference between suction side and pressure side is the loading of the profile. The integral of this loading distribution over the chord gives the lift force L on the profile. The lift coefficient can be given as:

$$C_L = \frac{L}{\frac{1}{2}\rho S V^2} \qquad (26)$$

where S is an area (span times chord length). For a profile the lift coefficient per unit span is also used where S is replaced by the chord length c. A typical angle of attack versus C_L is shown in the figure below
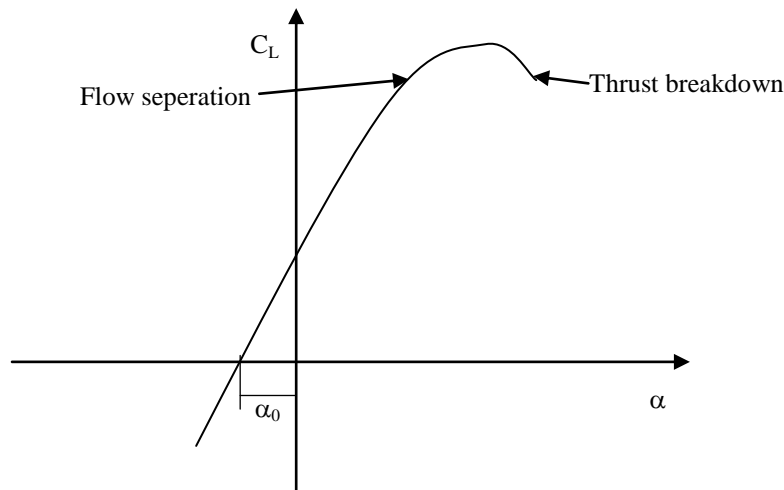
As can be seen in the above figure the lift coefficient C_L crosses the x-axis at the zero lift angle (α_0) where the profile generates no lift. This angle is determined by the camber of the profile and calculated as $\alpha_0 = \frac{2 f_{max}}{c}$. The slope of the lift curve ($\frac{\partial C_L}{\partial \alpha}$) is 2π for thin profiles. So that the lift coefficient of a thin profile can be written as:

$$C_L = 2\pi(\alpha + \alpha_0) \qquad (27)$$

At higher angles of attack the lift curve deviates from the linear theory and flow separation and thrust breakdown occur.

The term ideal angle of attack, α_i, is the angle of attack at which pressure around the leading edge is symmetrical In this case the flow direction at the leading edge is exactly in the direction of camber line. It is very important because at this angle the pressure close to the leading edge is maximum. Propeller blade sections are generally designed to operate at the ideal angle of attack.

The drag force is caused by the friction along the surface of the profile and is expressed in non-dimensional terms as:

$$C_D = \frac{D}{\frac{1}{2}\rho S V^2}$$

(28)

d) Profile Series

National Advisory Committee for Aeronautics (NACA) produced and tested a large number of profiles (aerofoils). All data of NACA foils are given in appropriate tables for two main forms: basic symmetrical thickness forms and mean line forms. Thickness and velocity distributions are given at zero lift angles for the basic symmetrical thickness forms and at ideal angles of attack for the mean line forms.

A foil desired by a designer's requirements can be chosen by combining a mean line and a thickness distribution that is perpendicular to the mean line or to the chord line as in practice.

According to NACA procedure, the pressure distribution around a NACA foil can be estimated as follows:

1- The velocity distribution (v/V) over the basic thickness form at zero lift angle is directly taken from the appropriate NACA table if the actual or desired foil has the same ratio of maximum thickness to chord length t/c given in the NACA series. If it does not, the values of (v/V) can be calculated using a linear scaling relationship given by the NACA:

$$\left(\frac{v}{V}\right)_{t_2} = \left[\left(\frac{v}{V}\right)_{t_1} - 1\right]\frac{t_2}{t_1} + 1$$

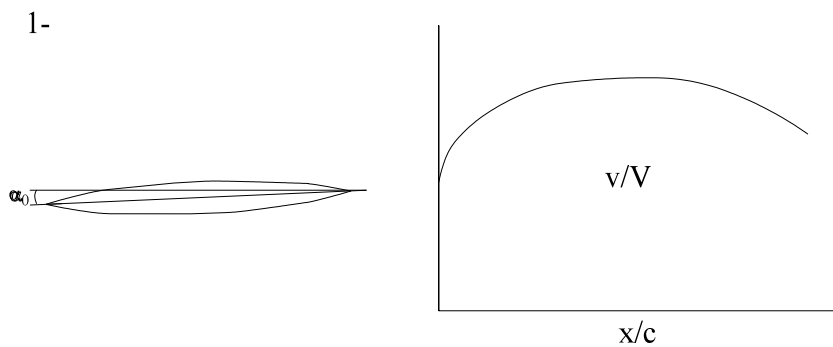where t_1 is the nearest thickness ratio given in the series and t_2 is the actual or desired thickness ratio.

1-

Figure 1 Symmetrical foil section at zero lift angle of attack.

2- Values of the load distribution of the mean line at its ideal angle of attack, (Δv/V), are directly read from the appropriate NACA table if the actual foil has the same camber to chord ratio f/c given in the series. If it does not have the same camber ratio the values of ideal lift coefficient C_{Li}, ideal angle of attack α_i, section moment coefficient about the quarter-chord point $c_{mc/4}$ and Δv/V distribution are scaled by a camber scale factor S_c:

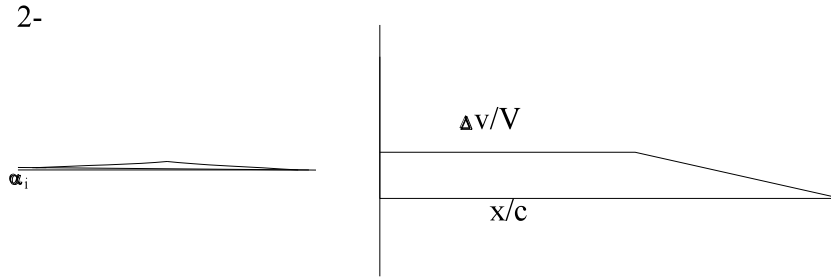$$S_c = \frac{(f/c) \text{ of the actual foil}}{(f/c) \text{ of the NACA series}}$$

2-

Figure 2. Mean line at ideal angle of attack

3- In this step, the pressure/velocity values devised in the step 1 and 2 are combined to obtain the required values for cambered foil at ideal angle of attack. (+) sign represents the upper part and (-) sign represents the lower part.
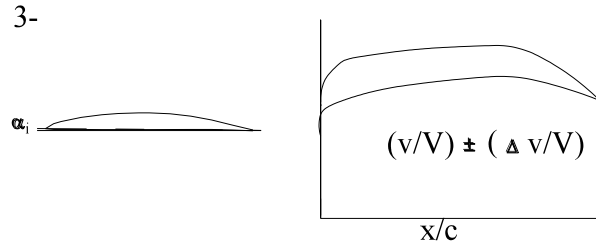
3-

Figure 3. Cambered foil section at ideal angle of attack

4- In this step, the values of the velocity increments $\Delta v_a / v$ (additional load distribution) induced by changing angle of attack are calculated such that: if the actual foil does not have the same thickness ratio given in the NACA series, the values of velocity increment $\Delta v_a/V$ are scaled by interpolating the values of $\Delta v_a/V$ in the NACA series by following relationship:

$$\left(\frac{\Delta v_a}{V}\right)_2 = \left(\frac{\Delta v_a}{V}\right)_1 + \left\{ \frac{\left(\frac{\Delta v_a}{V}\right)_3 - \left(\frac{\Delta v_a}{V}\right)_1}{t_3 - t_1} \right\}(t_2 - t_1)$$

where subscripts 1 represents the NACA data for the thickness ratio given in the NACA series smaller than the thickness of the actual foil, 2 represents the actual foil and 3 represents the NACA data for the thickness ratio given in the NACA series bigger than the thickness of actual foil.
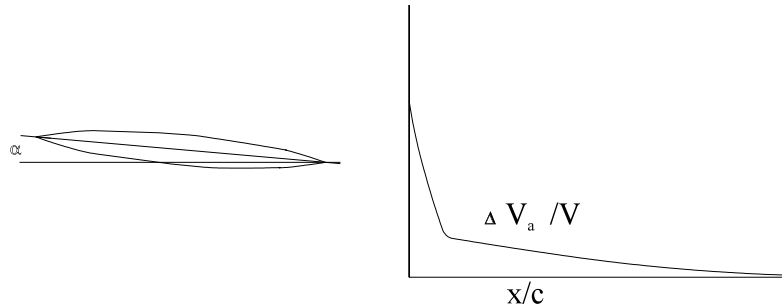

Figure 4. Velocity increment resulting from angle of attack for symmetrical foil section

These values of velocity increment in the NACA series were originally calculated at an additional lift coefficient of approximately unity. It must, therefore, be noted that they must be scaled by the additional scale factor given by:

$$S_A = \frac{\alpha - \alpha_i}{\alpha_g} \quad \text{or } S_A = \frac{C_L - C_{Li}}{C_{Lg}}$$

where C_L is the desired lift coefficient, C_{Li} is the ideal lift coefficient, C_{Lg} is the lift coefficient for which the values of $\Delta v_a/V$ were originally calculated, α is the desired angle of attack, α_i is the ideal angle of attack, α_g is the angle of attack for which the values of $\Delta v_a/V$ were originally calculated.

5- Velocity distributions at upper and lower parts at an angle of attack are calculated by following relationships:

$$\left(\frac{v}{V}\right)_U = \frac{v}{V} + S_c \frac{\Delta v}{V} + S_A \frac{\Delta v_a}{V} \quad \text{on upper(back) part}$$

$$\left(\frac{v}{V}\right)_L = \frac{v}{V} - S_c \frac{\Delta v}{V} - S_A \frac{\Delta v_a}{V} \quad \text{on lower(face) part}$$

where the subscript U represents upper part and the subscript L represents lower part of foil.
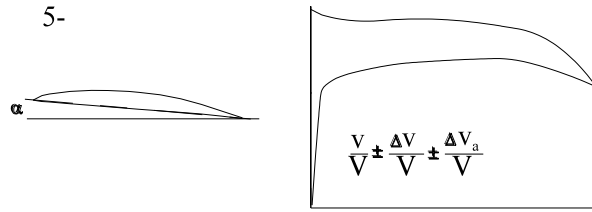
5-

Figure 5. Cambered foil section at angle of attack

6- Pressure distribution in terms of non-dimensional pressure coefficient C_p is calculated on both sides:

$$\left(C_p\right)_U = 1 - \left(\frac{v}{V}\right)^2_U \quad \text{and} \quad \left(C_p\right)_L = 1 - \left(\frac{v}{V}\right)^2_L$$

NACA has families of sections:

 a) 4-digit sections
 b) 5-digit sections
 c) 1 – series
 d) 6 – series
 e) 7 – series

For example: NACA four digit sections are designated as:

NACA 2415

First integer (2) denotes the maximum value of the mean line ordinate in percentage of the chord 100(fmax/c).

Second integer (4) denotes the position of maximum camber (fmax) in tenths of the chord from the leading edge.

Las two integers (15) denote the maximum thickness in percentage of the chord 100(tmax/c).

In this case NACA 2415 section has 2 per cent camber at 0.4 of the chord from the leading edge and 15 per cent thickness.

e) Lifting Line Theory

A simple solution for unswept three-dimensional wings can be obtained by using Prandtl's lifting line model. For incompressible, inviscid flow, the wing is modelled as a single bound vortex line located at the 1/4 chord position and an associated shed vortex sheet.
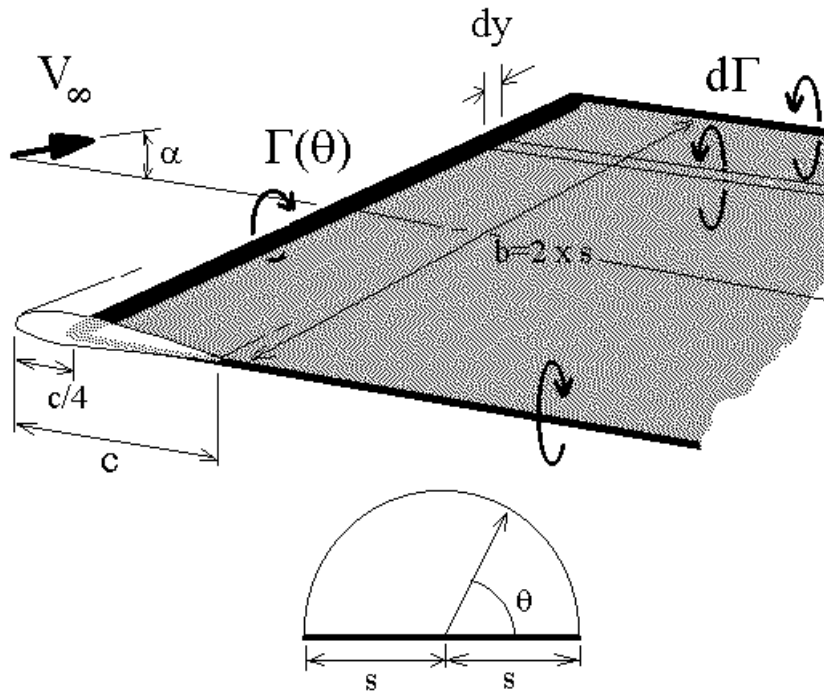
The span-wise lift distribution is assumed to be elliptical with a small modification due to wing planform geometry. The assumed vortex line strength is thus a Fourier series approximation.

$$\Gamma(y) = \Gamma(\theta) = 4sV_\infty \sum_{n=1}^{\infty} A_n \sin(n\theta) \qquad (29)$$

The required strength of the distribution coefficients (A_n) for a given geometry and set of free-stream conditions can be calculated by applying a surface flow boundary condition. The equation used is based on the usual condition of zero flow normal to the surface. For 3-D wings the condition is applied at several span-wise sections by matching flow and surface angles. The local flow angle of incidence for a 2-D section of the wing must be equal to the sum of the wing's angle of attack, the section twist and the downwash induced flow angle. This downwash component is caused by the induced flow from the trailing vortex sheet.

$$\alpha_{2\text{-}D} = \alpha - \alpha_i + \theta_t$$
$$\alpha_i = w_i / V_\infty$$

12
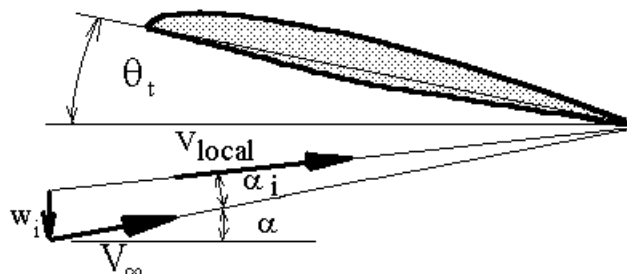
where α is the 3-D wing angle of attack, θ_t is the wing twist angle and w_i is the velocity induced by trailing vortex sheet.

The vortex strength distribution in the trailing sheet will be a function of the changes in vortex strength along the wing span. The mathematical function describing the vortex sheet strength is thus obtained by differentiating the bound vortex distribution.

$$d\Gamma = 4sV_\infty \sum_{n=1}^{\infty} nA_n \cos(n\theta).d\theta \qquad (30)$$

A solution for the magnitude of the Fourier coefficients $A_1, A_2, A_3...$ is obtained by firstly predicting the downwash velocity induced on the wing by the trailing sheet.

$$w_i = \frac{1}{4}\pi \int_{-s}^{+s} \frac{d\Gamma}{(y-y_i)} = V_\infty \sum_{n=1}^{\infty} \frac{nA_n \sin(n\theta)}{\sin(\theta)} \qquad (31)$$

Then find the 2-D section lift coefficient as a function of the local flow incidence and the bound vortex strength at this span location.

$$C_l = a_o(\alpha_{2D} - \alpha_o) = \frac{2\Gamma}{V_\infty c} \qquad (32)$$

where a_o is the section lift curve slope $(\partial C_l/\partial \alpha)$, α_o is the zero lift angle and c is the section chord.

Rearranging and substituting for the local angle of incidence.

$$\Gamma = \frac{1}{2}a_o V_\infty c(\alpha - \alpha_i + \theta_t - \alpha_o) \qquad (33)$$

Substituting for Γ and α_i in terms of the Fourier series approximations then a final boundary condition equation is obtained. The equation contains the unknown coefficients and the known geometric properties of the wing.

$$\sum_{n=1}^{\infty} A_n \sin(n\theta) \left[\sin(\theta) + n\frac{a_o c}{8s} \right] = \frac{a_o c}{8s} \sin(\theta)(\alpha + \theta_t - \alpha_o) \qquad (34)$$

If a fixed number of coefficients $(A_1,A_2,A_3,A_4...A_N)$ is used then a set of simultaneous linear equations will be obtained by applying the above equation at "N" spanwise locations. A cosine distribution of spanwise locations should be used to match the assumed wing loading distribution. The number of coefficients used will determine the accuracy of the solution. If the wing loading is highly non-elliptical then a larger number of coefficients should be included. The solution for coefficients $(A_1,A_2,A_3,A_4...A_N)$ is obtained by the reduction of the resulting matrix of equations.

It should be noted that in cases were the wing loading is symmetric then even coefficients $(A_2,A_4,A_6,....)$ will be zero and can be deleted from the calculation.

The lift coefficient for the wing at a given angle of attack will be obtained by integrating the spanwise vortex distribution.

$$L = \rho V_\infty \int_{-s}^{+s} \Gamma dy \tag{35}$$

so that $C_L = \pi .AR.A_1$, where AR is wing aspect ratio.

The downwash velocity induced at any span location can be calculated once the strength of the wing loading is known. The variation in local flow angles can then be found. A consequence of this downwash flow is that the direction of action of each section's lift vector is rotated relative to the free-stream direction. The local lift vectors are rotated backward and hence give rise to a lift induced drag. By integrating the component of section lift coefficient that acts parallel to the free-stream across the span, the induced drag coefficient can be found.

$$D_i = \rho V_\infty \int_{-s}^{+s} \Gamma \sin(\alpha_i) dy \tag{36}$$

so that $C_{Di} = \pi .AR.\Sigma (nA_n^2)$

No real information about pitching moment coefficient can be deduced from lifting line theory since the lift distribution is collapsed to a single line along the 1/4 chord.
Special case of elliptical loading:

If the wing planform is elliptical, then it can be assumed that the wing load distribution is also a purely elliptical function.

$$\Gamma (y) = 4sV\infty A_1\sin(\theta) = \Gamma_o\sin(\theta) \tag{37}$$

In this case a single general boundary condition equation results containing only one unknown, the vortex line strength at the wing root. The exact solution of this equation leads to the following simple answer for lift coefficient and induced drag coefficient.

$$\frac{\partial C_L}{\partial \alpha} = \frac{a_o}{\left(1 + \dfrac{a_o}{\pi AR}\right)} \tag{38}$$

$$C_{Di} = \frac{C_L^2}{\pi .AR} \tag{39}$$

$$\alpha_{o(2D)} = \alpha_{o(3D)}$$

f) Lifting Surface Theory

If the aspect ratio ($AR = \dfrac{b^2}{A} = \dfrac{b}{c}$) of blades is high, and if the rake and skew is zero (or at least small), the lifting line theory is applicable. The lifting line method works well for conventional airplane propellers, which have straight radial blades of very

high aspect ratio. However, it is not suitable for marine propellers. Therefore lifting surface theory was introduced to overcome the above difficulties.

In the lifting surface theory, the real propeller geometry is dealt. The blade mean surface is defined in terms of a camber distribution. Thickness is added symmetrically with respect to mean line at each radius.

g) Boundary Element Methods

Boundary element methods, which are also known as **"Panel Methods"**, are based on the approach developed by Hess and Smith (1967). In these methods, the surfaces of propeller blades and hub or foil surface are discretised by a number of small quadrilateral panels having constant source and doublet distributions. The trailing vortex sheet is also represented by similar quadrilateral panels having constant doublet distributions. The strengths of the source and doublet distributions are determined by solving the boundary value problems at each of the control points, which are located on each panel. They are inherently **"Non-linear"** with either the thickness or the angle of attack, since they make no assumption about the magnitude of these quantities. On the other hand, the panel methods become very expensive, in terms of computing time, in the case of three-dimensional geometries (marine propellers) as the number of panels are increased tremendously compared to the 2-D foils.